Tissue Engineering

DOI: 10.1089/ten.TEA.2021.0209

Bile duct regeneration with an artificial bile duct made of gelatin hydrogel non-woven fabrics

Yusuke Uemoto[1,2], Kojiro Taura[1], Daichi Nakamura[1], Li Xuefeng[1], Nguyen Hai Nam[1], Yusuke Kimura[1], Kenji Yoshino[1,3], Hiroaki Fuji[1], Tomoaki Yoh[1], Takahiro Nishio[1], Gen Yamamoto[1], Yukinori Koyama[1], Satoru Seo[1], Tatsuaki Tsuruyama[4], Keiko Iwaisako[5], Shinji Uemoto[6], Yasuhiko Tabata[2], Etsuro Hatano[1]

[1] Division of Hepato-Biliary-Pancreatic Surgery and Transplantation, Department of Surgery, Graduate School of Medicine, Kyoto University, Kyoto, Japan

[2] Laboratory of Biomaterials, Department of Regeneration Science and Engineering, Institute for Frontier Life and Medical Sciences, Kyoto University, Kyoto, Japan.

[3] Department of Surgery, Nagahama City Hospital, Nagahama, Japan

[4] Clinical Bioresource Center, Kyoto University Hospital, Kyoto, Japan

[5] Department of Medical Life Systems, Faculty of Life and Medical Sciences, Doshisha University, Kyotanabe, Japan

[6] Shiga University of Medical Science, Otsu, Japan

*Correspondence to: Kojiro Taura

Division of Hepato-Biliary-Pancreatic Surgery and Transplantation, Department of Surgery, Kyoto University Graduate School of Medicine

54 Kawaharacho, Shogoin, Sakyo-ku, Kyoto, Japan

Tel: +81-75-751-3242; Fax: +81-75-751-4263

e-mail: ktaura@kuhp.kyoto-u.ac.jp

Yusuke Uemoto

e-mail: uemoto6001@kuhp.kyoto-u.ac.jp

Tel: +81-75-751-3242

54 Kawaharacho, Shogoin, Sakyo-ku, Kyoto, Japan

Daichi Nakamura

e-mail: daichinaka@kuhp.kyoto-u.ac.jp

Tel: +81-75-751-3242

54 Kawaharacho, Shogoin, Sakyo-ku, Kyoto, Japan

Li Xuefeng

e-mail: lixuefeng2017@yahoo.co.jp

Tel: +81-75-751-3242

54 Kawaharacho, Shogoin, Sakyo-ku, Kyoto, Japan

Nguyen Hai Nam

e-mail: dr.nguyenhainam@gmail.com

Tel: +81-75-751-3242

54 Kawaharacho, Shogoin, Sakyo-ku, Kyoto, Japan

Yusuke Kimura

e-mail: ykimura@kuhp.kyoto-u.ac.jp

Tel: +81-75-751-3242

54 Kawaharacho, Shogoin, Sakyo-ku, Kyoto, Japan

Tissue Engineering
Bile duct regeneration with an artificial bile duct made of gelatin hydrogel non-woven fabrics (DOI: 10.1089/ten.TEA.2021.0209)

Kenji Yoshino

e-mail: kenji.yoshino1980@gmail.com

Tel: +81-749-68-2300

313 Oinuicho, Nagahama, Shiga, Japan

Hiroaki Fuji

e-mail: fhiro@kuhp.kyoto-u.ac.jp

Tel: +81-75-751-3242

54 Kawaharacho, Shogoin, Sakyo-ku, Kyoto, Japan

Tomoaki Yoh

e-mail: tomyoh@kuhp.kyoto-u.ac.jp

Tel: +81-75-751-3242

54 Kawaharacho, Shogoin, Sakyo-ku, Kyoto, Japan

Takahiro Nishio

e-mail: tnishio@kuhp.kyoto-u.ac.jp

Tel: +81-75-751-3242

54 Kawaharacho, Shogoin, Sakyo-ku, Kyoto, Japan

Gen Yamamoto

e-mail: genymmt@kuhp.kyoto-u.ac.jp

Tel: +81-75-751-3242

54 Kawaharacho, Shogoin, Sakyo-ku, Kyoto, Japan

Tissue Engineering
Bile duct regeneration with an artificial bile duct made of gelatin hydrogel non-woven fabrics (DOI: 10.1089/ten.TEA.2021.0209)

Yukinori Koyama

e-mail: ykoyama@kuhp.kyoto-u.ac.jp

Tel: +81-75-751-3242

54 Kawaharacho, Shogoin, Sakyo-ku, Kyoto, Japan

Satoru Seo

e-mail: rutosa@kuhp.kyoto-u.ac.jp

Tel: +81-75-751-3242

54 Kawaharacho, Shogoin, Sakyo-ku, Kyoto, Japan

Tatsuaki Tsuruyama

e-mail: tsuruyam@kuhp.kyoto-u.ac.jp

Tel: +81-75-366-7646

54 Kawaharacho, Shogoin, Sakyo-ku, Kyoto, Japan

Keiko Iwaisako

e-mail: iwaisako@kuhp.kyoto-u.ac.jp

Tel: +81-774-65-6020

1-3 Tataramiyakodani, Kyotanabe, Kyoto, Japan

Shinji Uemoto

e-mail: uemoto@kuhp.kyoto-u.ac.jp

Tel: +81-77-548-2111

Seta Tsukinowa-cho, Otsu, Shiga, Japan

Tissue Engineering
Bile duct regeneration with an artificial bile duct made of gelatin hydrogel non-woven fabrics (DOI: 10.1089/ten.TEA.2021.0209)

Yasuhiko Tabata

e-mail: yasuhiko@infront.kyoto-u.ac.jp

Tel: +81-75-751-4128

53 Kawaharacho, Shogoin, Sakyo-ku, Kyoto, Japan

Etsuro Hatano

e-mail: etsu@kuhp.kyoto-u.ac.jp

Tel: +81-75-751-3242

54 Kawaharacho, Shogoin, Sakyo-ku, Kyoto, Japan

Running head: ABD OF GELATIN HYDROGEL

Keywords: artificial bile duct, gelatin, regenerative medicine

The results of this research will be presented at the 43rd Japanese Society for Biomaterials and 8th Asian Biomaterials Congress (November 28-30, 2021, Nagoya Congress Center, Japan).

Tissue Engineering
Bile duct regeneration with an artificial bile duct made of gelatin hydrogel non-woven fabrics (DOI: 10.1089/ten.TEA.2021.0209)

Abstract

Although choledochojejunostomy is the standard technique for biliary reconstruction, there are various associated problems that need to be solved such as reflux cholangitis. Interposition with an artificial bile duct (ABD) to replace the resected bile duct maintains a physiological conduit for bile and may solve this problem. This study investigated the usefulness of an ABD made of gelatin hydrogel non-woven fabric (GHNF). GHNF was prepared by the solution blow spinning method. The migration and activity of murine fibroblast L929 cells were examined in GHNF sheets. L929 cells migrated into GHNF sheets, where they proliferated and synthesized collagen, suggesting GHNF is a promising scaffold for bile duct regeneration. ABDs made of GHNF were implanted in place of resected bile duct segments in rats. The rats were sacrificed at 2, 6, and 12 weeks post-implantation. The implantation site was histologically evaluated for bile duct regeneration. At postoperative 2 weeks, migrating cells were observed in the ABD pores. The implanted ABD was mostly degraded and replaced by collagen fibers at 6 weeks. Ki67-positive bile duct epithelial cells appeared within the implanted ABD. These were most abundant within the central part of the ABD after 6 weeks. The percentages of Ki67-positive cells were 31.7%±9.1% in the experimental group and 0.8%±0.6% in the sham operation group at 6 weeks ($p<0.05$), indicating that mature biliary epithelial cells at the stump proliferated to regenerate the biliary epithelium. Biliary epithelial cells had almost completely covered the bile duct lumen at 12 weeks (epithelialization ratios: 10.4%±6.9% at 2 weeks, 93.1%±5.1% at 6 weeks, 99.2%±1.6% at 12 weeks). The regenerated epithelium was positive for the bile duct epithelium marker cytokeratin 19. Bile duct regeneration was accompanied by angiogenesis, as evidenced by the appearance of CD31-positive vascular structures. Capillaries were induced 2 weeks after implantation. The number of capillaries reached a maximum at 6 weeks and decreased to the same level as that of normal bile ducts at 12 weeks. These results showed that an ABD of GHNF contributed to successful bile duct regeneration in rats by facilitating the cell migration required for extracellular matrix synthesis, angiogenesis, and epithelialization.

Impact Statement

Development of an artificial bile duct enables physiological biliary reconstruction and may solve clinical problems associated with choledochojejunostomy. In this study, we created artificial bile ducts with gelatin hydrogel non-woven fabric and implanted them in place of resected bile duct in rats. We evaluated the process of bile duct regeneration as well as decomposition of the artificial bile duct and demonstrated successful regeneration of resected bile duct, highlighting the possibility of this novel biliary reconstruction method to replace choledochojejunostomy.

Tissue Engineering
Bile duct regeneration with an artificial bile duct made of gelatin hydrogel non-woven fabrics (DOI: 10.1089/ten.TEA.2021.0209)

Introduction

Bile duct resection is performed as a surgical treatment for various biliary disorders such as cholangiocarcinoma, congenital biliary dilatation, and benign biliary strictures resulting from trauma, Mirrizi syndrome, or iatrogenic bile duct injury. Choledochojejunostomy is the standard technique of biliary reconstruction after bile duct resection; however, it is associated with various problems that need to be overcome including the complexity of the procedure, risk of anastomotic leakage and stenosis, reflux cholangitis, and carcinogenesis.[1, 2] Additionally, endoscopic intervention in the anastomotic site or intrahepatic bile duct becomes more challenging after choledochojejunostomy.

Interposition of an artificial bile duct (ABD) in place of the resected extrahepatic bile duct could reconstruct the physiological biliary tract, which may solve the various problems associated with choledochojejunostomy. Attempts at developing ABD have been made for a long time.[3] Autologous tissue,[4, 5] non-degradable materials, and degradable materials have been used as ABD materials.[6-8] However, an ABD has not been successfully put into clinical use yet. This is in contrast to the fact that artificial blood vessels have been in practical use for decades and are indispensable for cardiovascular surgery.

Gelatin is a natural macromolecule consisting of collagen that has good biocompatibility, degradability, and low immunogenicity. Gelatin has been used clinically as a temporal embolization material (Spongel® or Gelpart®), making it advantageous when considering clinical applications. We have recently developed non-woven fabrics made of gelatin (gelatin hydrogel non-woven fabrics [GHNF]) and demonstrated their utility as scaffolds that facilitate cell migration and maintain cellular functions.[9] Thus, we expect GHNF to be promising materials for ABD. In this study, we generated an ABD using GHNF and evaluated its feasibility for biliary reconstruction in a rat model.

Materials and methods

1. Preparing the GHNF and polypropylene non-woven fabric (PPNF) sheets and ABD

The GHNF and PPNF sheets and ABD made of GHNF were supplied by The Japan Wool Textile Co., Ltd (Hyogo, Japan). GHNF sheets were prepared by the previously reported solution blow spinning method.[9] Polypropylene (PP) was selected as a control for the in

vitro experiments because PP has a cell adhesion capacity and structural characteristics (fiber diameter and density) similar to those of GHNF when processed into a non-woven fabric. The GHNF sheet was punched out into disks of 8 mm in diameter and the PPNF sheet was punched out into disks of 11 mm in diameter. The ABD was made by the same method as the GHNF with some modifications. To acquire sufficient strength for anastomosis, the density was increased by spinning at a speed approximately 18-fold faster than for GHNF sheet preparation and keeping in wet during lamination. The gelatin density of the GHNF and the ABD were 0.26±0.01 mg/mm^3 and 0.73±0.03 mg/mm^3, respectively. All biomaterials were sterilized with ethylene oxide gas.

2. Measuring the material properties of GHNF and PPNF sheets and ABD

The weight of the dry and swollen GHNF, and the volume of swollen GHNF were measured. The porosity of GHNF was calculated by the following formula: {(WGHNF – WG) ÷ VGHNF} × 100 (%), where WGHNF is weight of swollen GHNF, WG is weight of swollen gelatin (calculated as 3.1-fold increase over the weight of dry GHNF), and VGHNF is volume of swollen GHNF. The porosity of the PPNF sheet was calculated in the same method. The density of polypropylene was 0.9 g/cm³. The fiber diameter was measured with the Image J program (Public Domain Image Processing Program, National Institutes of Health, Bethesda, MD, USA) from an image taken with an optical microscope (BZ-X710; Keyence Co. Ltd., Tokyo, Japan). The stiffness of swollen GHNF sheets and ABD were measured with a creep meter (RE2-33005C; Yamaden, Bunkyo-ku, Tokyo, Japan). Stress was measured up to a strain of 50%.

3. Fibroblast culture

Murine fibroblast L929 cells were cultured in Dulbecco's Modified Eagle Medium (Thermo Fisher Scientific, Waltham, MA, USA) supplemented with 10% fetal bovine serum (Thermo Fisher Scientific) and 1% penicillin/streptomycin (Nacalai Tesque, Kyoto, Japan) at 37°C. L929 cells at 90% confluence were detached with 0.25% trypsin-EDTA (Nacalai Tesque) to obtain a cell suspension.

4. Preparing fibroblast aggregates for migration assays on GHNF sheets and ABD

Cell aggregates were prepared as described by Nii *et al*.[10] Briefly, the L929 cell suspension (5×10^3 cells/mL, 200 µL) was seeded onto a polyvinyl alcohol (degree of polymerization:

1800; saponification: 88 mol%; Unichika, Tokyo, Japan)-coated round-bottomed 96-well plate and cultured for 3 d to prepare cell aggregates.

The prepared aggregates were seeded onto swollen GHNF sheets, cultured, and then collected at the designated timepoints (12, 24, 48, and 72 h). Similarly, cell aggregates were seeded onto the ABD, and then collected at the same timepoints.

5. Cell culture in the GHNF and PPNF sheets and ABD

A L929 cell suspension (10×10^6 cells/mL, 20 µL) were seeded onto swollen GHNF and PPNF sheets with 0.1 mM L-ascorbic acid phosphate magnesium (FUJIFILM Wako Pure Chemical Co., Osaka, Japan). Cells were cultured statically for 2 d and with swirling at 90 rpm using an orbital shaker (Bellco Biotechnology, Vineland, NJ, USA) for 5 d. The medium was changed every 2 to 3 d. For the experiments involving ABD, cells were seeded by dipping dry ABD in a cell suspension (10×10^6 cells/mL). The cells were incubated statically for 2 d and with swirling at 90 rpm for 5 and 12 d.

6. ABD implantation in model rats

Female Sprague-Dawley rats (Charles River, Kanagawa, Japan) weighing 260±11.8 g were used in this experiment. The animals were anesthetized by inhaling 1.5% isoflurane. Blood samples were collected from the tail vein. Abdominal midline laparotomy was performed, and the common bile duct was exposed. A 1 to 2 mm segment of the common bile duct was resected. Each stump of the bile duct and swollen ABD (4-mm in length) were anastomosed with 10-0 nylon (Crownjun, Ichikawa, Chiba, Japan) under a microscope. A polyethylene tube (SP-8; Natsume, Yushima, Tokyo, Japan) was placed as a stent in the lumen. In the sham group, only abdominal midline laparotomy was performed after blood sampling from the tail vein. Rats were fed a standard chow diet with free access to tap water. ABD group rats were sacrificed at 2, 6, and 12 weeks after implantation, and the sham group rats were sacrificed at 12 weeks. Blood samples were collected from the tail vein and the inferior vena cava, and the bile duct was collected. The institutional animal research committee of Kyoto University approved this experimental protocol (Medkyo-19170). All experiments were conducted in accordance with the Guidelines for the Care and Use of Laboratory Animals from the National Institutes of Health.

7. Histology

Cell aggregates on GHNF sheets and ABD were fixed with a 4% paraformaldehyde (PFA) solution, embedded in optimal cutting temperature compound, and frozen. Frozen samples were cut into 6-µm thick sections by a cryotome (CM3050S; Leica Microsystems, Wetzlar, Germany). Hematoxylin and eosin (HE) staining was performed on each sample. Bile ducts were harvested from all rats used in the animal experiments, fixed with a 4% PFA solution, embedded in paraffin, and sectioned into 4-µm thick sections. HE staining was performed on each sample. Prepared specimens were examined under an optical microscope.

8. Sirius red staining

Sections of frozen tissue were stained with the Sirius Red/Fast Green Collagen Staining Kit (Chondrex, Woodinville, WA, USA), and sections of paraffin-embedded tissue were stained with the staining solution (Sirius Red 500 mg/Van Gieson solution P, 500 mL).

9. Immunofluorescence

After permeabilization and blocking, sections were incubated overnight at 4°C with primary antibodies. Then the sections were incubated for 1 h with labeled isotype-specific secondary antibodies (AlexaFluor, Invitrogen, Life Technologies Ltd, Paisley, UK) and counterstained with 4,6-diamidino-2-phenylindole (DAPI). The antibodies used for immunofluorescence are described in **Supplementary Table S1**.

10. Immunohistochemistry

After deparaffinization, antigen retrieval and blocking of endogenous peroxidase activity were performed. Sections were incubated overnight at 4°C with primary antibodies, incubated with horseradish peroxidase-labeled polymer (Agilent Technologies, Santa Clara, CA, USA) for 20 min, colored with 3,3’-diaminobenzidine (Agilent Technologies), and counterstained with hematoxylin. The antibodies used for immunofluorescence are described in **Table S1**.

11. Quantitative real-time PCR (qPCR)

L929 cells cultured in GHNF sheets for 1 week were collected and total RNA was extracted with the RNeasy Plus Mini Kit (QIAGEN, Hilden, Germany) according to the manufacturer’s

instructions. Total RNA was reverse transcribed to complementary DNA using a high-capacity complementary DNA reverse transcription kit (Applied Biosystems, Foster City, CA, USA). The mRNA levels were analyzed by qPCR using a SYBR green master reaction mix on a StepOnePlus system (Applied Biosystems). β-actin was used for standardization. The primer sequences used for qPCR are listed in **Supplementary Table S2**. A calibration curve was prepared with the control samples, and a relative quantification method was performed. The control group was statically cultured L929 cells in medium supplemented with ascorbic acid on the polyethylene dish for 3 d.

12. Imaging and quantification of histology

To quantify the number of migrating cells into GHNF sheets from aggregates, the number of cells in the scaffold was counted using Image J **(Supplementary Fig S1a)**. To quantify cell localization within the GHNF and PPNF sheets, a cross section of the samples was divided into outside and inside area, and the cell localized area was quantified using Image J **(Supplementary Fig S1b)**. The bile duct regeneration ratio was calculated by the following formula: {(4 – a) ÷ 4} × 100 (%), where 4 is the length of the implanted artificial bile duct, and a is the distance of bile duct epithelial defect.

To quantify the number of capillaries, five high-power magnification (400×) images of CD31 immunohistochemical staining were taken. The number of capillaries were counted, and the CD31 positive area was analyzed by Image J. The number of Ki67 positive cells were also quantified in the same manner.

13. Statistical analysis

All data are presented as mean ± standard deviation. Differences between groups were compared using the Mann–Whitney U test. A P-value <0.05 was considered statistically significant. JMP Pro 14 software (SAS institute, Cary, NC, USA) was used for all statistical analyses.

Results

1. Measurements of the structural parameters of GHNF sheets

The macroscopic appearance of GHNF sheets in the dry and saturated swollen states are shown in **Figs. 1a and b**, respectively. The swelling ratio of GHNF sheets, which was

calculated as the weight of the swollen GHNF sheet divided by the weight of the dry GHNF sheet, was 10.1±0.05. The porosity of GHNF sheets was 66.7%±4.4%. The microscopic appearance of a GHNF sheet is shown in **Fig. 1c**. The mean fiber diameter of the GHNF sheet was 48.7±6.6 μm. When the stiffness of the GHNF sheet was measured by creep mater, the stress was 7.6±1.4 kPa at 30% strain and 20.6±2.7 kPa at 50% strain.

2. Migration assays on GHNF sheets

Migration assays were performed to investigate if gelatin hydrogel was a suitable environment for cell infiltration. When L929 cell aggregates were seeded onto GHNF sheets, the cells migrated into the GHNF sheet around the cell aggregates **(Fig. 2a)**. The number of cells that migrated into the GHNF sheet increased over time **(Fig. 2b)**. The cells migrating into the GHNF sheet were positive for Ki67, demonstrating that they maintained proliferative ability **(Fig. 2c)**. L929 cells cultured in GHNF sheets had higher collagen mRNA expression than those cultured on plastic dishes **(Fig. 2d)**.

3. Comparing the localization of cells cultured in GHNF and PPNF sheets

We next evaluated whether cells were present inside the GHNF sheet. PPNF sheets with similar porosity (61.4%±0.87%) and fiber diameter (49.4±5.6 μm) were used as a control **(Fig. 3a)**. Cells proliferated in both the GHNF and PPNF scaffolds, but there were significantly more cells present inside the GHNF sheet than the PPNF sheet **(Fig. 3b, c)**. The diffusion limit of oxygen and nutrients made the culture conditions worse inside the scaffold than the surface. The presence of more cells inside the GHNF sheet suggested that the GHNF sheet had advantages over PPNF in terms of cell survival.

4. Measuring the stiffness of GHNF sheets, ABD, and the structural parameters of ABD

After confirming the suitability of GHNF sheets as a scaffold that induces cell migration, we created an ABD using GHNF. As the GHNF sheets used in previous experiments were not strong enough for anastomosis (data not shown), the ABD was prepared with an increased gelatin density. The macroscopic appearance of the ABD is shown in **Fig. 4a**. The swollen ABD had an inner diameter of 0.8 mm and a wall thickness of 1.0 to 1.1 mm. When compressed with the creep meter, the ABD showed a stress of approximately 8.5-fold greater than that of the GHNF sheet at 30% strain and approximately 9.4-fold greater than that of the GHNF sheet at 50% strain, indicating greater strength than the GHNF sheet. The

ABD was not easily torn and had sufficient strength for anastomosis (data not shown). The swelling ratio of the ABD was 4.6±0.12. The porosity of the ABD was 23.6%±1.25%. The microscopic findings of the ABD are shown in **Fig. 4a**. The fiber diameter of the ABD was 40.6±5.5 μm.

5. Cell migration and maintenance of cellular functions in the ABD

Similar experiments were performed to verify whether the characteristics of the GHNF sheet were maintained in the ABD, which had a higher density and lower porosity than the GHFN sheet. The cell aggregate was seeded onto the ABD in the same manner as the GHNF sheet. The number of the cells that migrated into the ABD increased over time, although it was decreased compared with the GHNF sheet **(Fig. 4b, c)**. The migrating cells in the ABD were Ki67 positive **(Fig. 4d)**, indicating a similar proliferation ability in ABD as in the GHNF sheet. When L929 cells were cultured for 1 week in ABD, collagen secretion (positive for Sirius red staining) was observed around the cells **(Fig. 4e)**. After culture for 2 weeks, the cells proliferated and the secreted collagen around the cells became more evident **(Fig. 4e)**, indicating that ability to synthesize extracellular matrix was maintained in ABD.

6. ABD implantation model in rats

Fig. 5a shows the gross appearance of the rat bile duct and a resected portion of the bile duct. ABD was interposed in place of the resected bile duct in the experimental group **(Fig. 5a)**. General status of the rats was maintained until sacrifice, as indicated by similar weight gain and serum biochemistry data as the sham group **(Table 1)**. **Figure 5b** shows the histological changes at the bile duct implantation site over time. Two weeks postoperatively, Sirius red staining revealed that most of the implanted ABD remained **(Fig. 5b(iii))**, and cells had migrated into pores of the ABD **(Fig. 5b(ii))**. Cytokeratin 19 (CK19) is one of the markers specific to bile duct epithelium.[11] The ABD was mostly not covered by bile duct epithelium, as indicated by few CK19-positive epithelial cells. At 6 weeks, the ABD was mostly degraded and replaced by collagen fibers **(Fig. 5b(iii))**. Epithelialization with CK19-positive bile duct epithelial cells was observed **(Fig. 5b(iv))**. CK19-positive epithelial cells were present on both ends and deficient in the center, suggesting that epithelialization initiated at the edges and progressed towards the center. At 12 weeks, epithelialization was almost completed, and the bile duct was thoroughly

regenerated. However, the bile duct epithelium showed a tall columnar shape, which was slightly different from the flat epithelium in the sham group. Epithelialization ratios at 2, 6, and 12 weeks were 10.4%±6.9%, 93.1%±5.1%, and 99.2%±1.6%, respectively **(Table 2)**.

7. Angiogenesis in the ABD of the rat implantation model

CD31 is expressed in vascular endothelial cells and is useful for evaluating vascular structure.[12] Two weeks after implantation, angiogenesis was observed in the ABD, as indicated by the presence of CD31-positive vascular structures **(Fig. 6a, b)**. Angiogenesis was most intense at 6 weeks post-implantation and decreased at 12 weeks compared with 6 weeks **(Fig. 6c)**. Capillaries of different sizes were formed at 6 weeks. On the other hand, at 12 weeks, the size difference of the capillaries was adjusted, and the thickness of endothelial cells was increased, and blood vessels with a stable structure were observed.

8. Proliferation of the biliary epithelium in the rat implantation model

Two weeks after implantation, few Ki67-positive bile duct epithelial cells were found (**Fig. 7a**). Many Ki67-positive cells were found 6 weeks after implantation and were abundant in the central part of the implantation site **(Fig. 7b)**. At 12 weeks post-implantation the number of Ki67 positive cells had decreased, suggesting that regeneration of the bile duct epithelium had passed the peak **(Fig. 7c)**.

Discussion

Biliary reconstruction using an ABD interposed in the excised part of the bile duct may solve various problems related to choledochojejunostomy such as reflux cholangitis. In this study, we demonstrated a successful regeneration of a neo-bile duct with an implanted ABD in rats. The process of degrading the implanted ABD and regenerating the bile duct was shown over time, which was corroborated by the capacity of the GHNF to accept cell migration *in vitro*.

In previous studies, various materials have been used for ABD including autologous tissue such as blood vessels and ureters[4, 5], non-degradable materials such as polytetrafluoroethylene[8], degradable materials such as polylactic acid and collagen[6, 7], and bioengineered materials.[13] Non-degradable materials have achieved limited success because they remain as foreign substances in the bile duct.[8] Autologous tissue and

bioengineered materials require extra time and effort for preparation. Degradable materials that permit cell migration and gradually decompose without leaving residuals in the bile duct appear to be the most convenient and promising for these purposes.

Gelatin is a biodegradable material that is enzymatically decomposed *in vivo* and used as various biomedical materials due to its high biocompatibility.[14] In previous studies, the biodegradable synthetic polymers polylactic acid (PLA) and polyglycolic acid (PGA) have been used for ABD.[6, 15] However, they generate acids upon degradation by hydrolysis, causing toxic pH changes.[16, 17] Degraded PLA particles could also cause inflammation.[18] Unlike PLA or PGA, gelatin is enzymatically degraded and does not cause inflammation. These characteristics prompted us to investigate the possibility of using gelatin as a substrate for ABD.

Fibroblasts play an essential role in wound healing by secreting extracellular matrix, especially collagen.[19] Thus the capacity of scaffolds to accept cell migration into their 3D structure is assumed to be an important requirement for successful bile duct regeneration. In this study, when fibroblast L929 cell aggregates were cultured on the GHNF sheet, the cells migrated from the cell aggregate into the sheet. The number of migrating cells into the deeper portion of the GHNF sheet was higher than that of the PPNF sheet, suggesting that the GHNF sheet permitted better oxygen and nutrients supply than the PPFN sheet.[20] Cell proliferation was observed in the GHNF sheet, as shown by Ki67 staining. Collagen mRNA expression was also detected and was even higher than that of the controls, possibly because of 3D culture. It has been reported that GHNF may reduce the diffusion limit of nutrients and oxygen.[9] Because the GHNF sheet contributed to more internal nutrients and oxygen supply, there were more cells inside the GHNF sheet compared with the PPNF sheet. Our data suggest that GHNF is a promising scaffold for bile duct regeneration in terms of cell migration, proliferation, and enhanced collagen synthesis. However, the GHNF sheet had insufficient anastomotic strength; thus, we prepared an ABD with increased gelatin density. The mechanical properties of this ABD were sufficiently improved for anastomosis. The porosity of ABD decreased in exchange for the increased strength; however, cell migration was also confirmed in the ABD by the migration assay.

Few studies using biodegradable materials have evaluated the process of degradation over time. Previous studies have demonstrated regeneration of the bile duct wall or bile duct epithelium was not achieved in 2 weeks[15] and required 6 weeks at the earliest.[6] As a preliminary experiment, we subcutaneously implanted GHNF in rats to evaluate its degradability with different thermal cross-linking conditions and found thermal cross-linking at 140℃ for 48 h was ideal (data not shown).

The ABD was successfully implanted in rats and appeared to function well without sign of cholestasis or liver dysfunction. Most of the past studies on ABD have shown only final status after bile duct regeneration was complete.[5, 8] Previous studies have not explored how the bile duct regenerated. In this study, we evaluated the degradation of the implanted ABD and regeneration of the bile duct over time. At 2 weeks after implantation, cell migration was observed in the ABD, which was in the process of degradation. At 6 weeks after implantation, the ABD was almost completely degraded, the wall of the bile duct was connected, and the bile duct epithelium appeared to regenerate from both sides of the bile duct stump. At 12 weeks after implantation, the bile duct epithelium uniformly covered the lumen. This histological transition suggested that the fibroblasts and bile duct epithelial cells necessary for bile duct regeneration had migrated from both sides of the artificial bile duct.

An adequate blood supply is essential for bile duct regeneration.[21] This study showed angiogenesis in the implanted ABD, as evidenced by CD31-positive ductular structures. This was achieved without the need for bioactive molecules, which are often used to induce angiogenesis in tissue engineering.[22, 23] Bioactive molecules are secreted by macrophages, neutrophils, fibroblasts, and others cell types.[24] It is speculated that the cells migrating into the ABD secret the angiogenic factors that induce blood vessels in the GHNF.[25]

An abundant expression of Ki67 in the biliary epithelium suggested interesting implications for the process of regeneration of the bile duct epithelium. Ki67 was highly expressed in the epithelium at 6 weeks after implantation and were concentrated near the center of the crypt with a tubular villous structure. This was very similar to the findings seen in the proliferative zone in the process of healing gastric ulcers.[26] Although little is

known about extrahepatic bile duct homeostasis and regeneration, a study on a bile duct injury model in mice suggested that the peribiliary glands were a stem cell niche for bile duct epithelium progenitors.[27] However, this study suggests that mature bile duct epithelium at the stump of the bile duct proliferated to regenerate the bile duct and questioned the need for bioengineered ABD as reported in the previous study.[28] Our hypothesis is supported by another previous study that showed no advantage in a bioengineered ABD compared with a simple ABD prepared from a biodegradable material.[6]

This study suggests that the GHNF ABD allows cells to migrate from both ends of anastomosis, which subsequently promoted extracellular matrix synthesis, angiogenesis, and epithelialization. It is possible that this series of events took place in synchronization with the degradation of ABD, resulting in successful bile duct regeneration.

There are some limitations to be acknowledged in this study. First, the length of the ABD used in our experiments was only 4 mm. Longer defects are expected to need more time for the bile duct to regenerate, raising a concern that the ABD used in our study may decompose too quickly. Second, in this present study, the bile duct stent was indwelled until sacrifice, so it has not been verified whether the patency is maintained after removal. We tried to establish a model in which the stent is removed after a few weeks but were unsuccessful because of technical difficulties. Third, we did not conduct a control in vivo experiment in which another material was utilized for the ABD. It would have been most appropriate to use PPNF as a control in the ABD implantation experiments as well as in the in vitro experiments. In fact, we performed preliminary experiments of subcutaneous implantation of GHNF and PPNF in rats. GHNF was mostly degraded at 4 weeks with no scar formation around the implant and no persistent inflammation. However, inflammatory cells were infiltrated around and inside the PPNF at 4 weeks (data not shown). We thought that the PPNF-induced inflammation may be due to its non-degradable nature, and thus it would not be suitable for ABD. On the basis of these findings, we did not perform a comparative experiment with PPNF in the ABD implant experiment, and the sham data were used as the control. Fourth, in rats, the gallbladder is not present and the sphincter of duodenal papilla is underdeveloped.[29] Because of these

anatomical differences, intraluminal pressure of the bile duct may be lower in rats than in humans,[30, 31] which may make anastomotic leakage less likely to occur in rats. Taking these limitations into consideration, verification in larger animals is needed before human testing.

Conclusion

In conclusion, we demonstrated successful bile duct regeneration in rats using an ABD made of GHNF. GHNF is a promising material for constructing ABD, and further research in larger animals is needed for future clinical applications.

Acknowledgments

The authors are grateful to The Japan Wool Textile Co., Ltd (Hyogo, Japan) for providing the GHNF sheets, PPNF sheets, and ABD. We also thank James P. Mahaffey, PhD, and H. Nikki March, PhD, from Edanz (https://jp.edanz.com/ac) for editing a draft of this manuscript.

Authors' contributions

Y. Uemoto, K. Taura, S. Uemoto, Y. Tabata, and E. Hatano were involved in the conception and design of study. Y. Uemoto, D. Nakamura, L. Xuefeng, N. H. Nam, Y. Kimura, K. Yoshino, and H. Fuji were involved in the acquisition of data. Y. Uemoto, K. Taura, T. Yoh, T. Nishio, G. Yamamoto, Y. Koyama, S. Seo, T. Tsuruyama, K. Iwaisako, and Y. Tabata were involved in the analysis and/or interpretation of data. Y. Uemoto and K. Taura were involved in the drafting the manuscript. Y. Tabata, and E. Hatano were involved revising the manuscript critically for important intellectual content. All authors critically revised the report, commented on drafts of the manuscript, and approved the final report.

Conflict of interest

Y. Uemoto and K. Taura receive research support of the providing materials from The Japan Wool Textile Co., Ltd in this research.

Y. Tabata receives research support from The Japan Wool Textile Co., Ltd.

All the other authors declare that they have no conflict of interest.

Funding

This research was supported by the Cooperative Research Program (Joint Usage/Research Center program) of the Institute for Frontier Life and Medical Sciences, Kyoto University, the Translational Research Seeds A 113 from the Japanese Agency for Medical Research and Development, and JSPS KAKENHI (Grant Number JP20K09006).

References

1. Panis Y, Fagniez PL, Brisset D, Lacaine F, Levard H, Hay JM. Long term results of choledochoduodenostomy versus choledochojejunostomy for choledocholithiasis. The French Association for Surgical Research. Surgery, gynecology & obstetrics. 1993;177(1):33-7.

2. Tocchi A, Mazzoni G, Liotta G, Lepre L, Cassini D, Miccini M. Late development of bile duct cancer in patients who had biliary-enteric drainage for benign disease: a follow-up study of more than 1,000 patients. Annals of surgery. 2001;234(2):210-4. doi:10.1097/00000658-200108000-00011.

3. Ginsburg N, Speese J. Autogenous fascial reconstruction of the bile duct. Annals of surgery. 1917;65(1):79-88. doi:10.1097/00000658-191701000-00007.

4. Capitanich P, Herrera J, Iovaldi ML et al. Bile duct replacement using an autologous femoral vein graft: an experimental study. Preliminary results. J Gastrointest Surg. 2005;9(3):369-73. doi:10.1016/j.gassur.2004.09.024.

5. Cheng Y, Xiong XZ, Zhou RX et al. Repair of a common bile duct defect with a decellularized ureteral graft. World J Gastroenterol. 2016;22(48):10575-83. doi:10.3748/wjg.v22.i48.10575.

6. Miyazawa M, Torii T, Toshimitsu Y, Okada K, Koyama I, Ikada Y. A tissue-engineered artificial bile duct grown to resemble the native bile duct. Am J Transplant. 2005;5(6):1541-7. doi:10.1111/j.1600-6143.2005.00845.x.

7. Nakashima S, Nakamura T, Han L-H et al. Experimental Biliary Reconstruction with an Artificial Bile Duct Using in situ Tissue Engineering Technique. Inflammation and Regeneration. 2007;27(6):579-85.

8. Gómez NA, Alvarez LR, Mite A et al. Repair of bile duct injuries with Gore-Tex vascular grafts: experimental study in dogs. J Gastrointest Surg. 2002;6(1):116-20. doi:10.1016/s1091-255x(01)00038-5.

9. Nakamura K, Saotome T, Shimada N, Matsuno K, Tabata Y. A Gelatin Hydrogel Nonwoven Fabric Facilitates Metabolic Activity of Multilayered Cell Sheets. Tissue Eng Part C Methods. 2019;25(6):344-52. doi:10.1089/ten.TEC.2019.0061.

10. Nii T, Makino K, Tabata Y. Influence of shaking culture on the biological functions of cell aggregates incorporating gelatin hydrogel microspheres. J Biosci Bioeng. 2019;128(5):606-12. doi:10.1016/j.jbiosc.2019.04.013.

11. Zong Y, Stanger BZ. Molecular mechanisms of liver and bile duct development. Wiley interdisciplinary reviews Developmental biology. 2012;1(5):643-55. doi:10.1002/wdev.47.

12. Muller WA, Ratti CM, McDonnell SL, Cohn ZA. A human endothelial cell-restricted, externally disposed plasmalemmal protein enriched in intercellular junctions. The Journal of experimental medicine. 1989;170(2):399-414. doi:10.1084/jem.170.2.399.

13. Zong C, Wang M, Yang F et al. A novel therapy strategy for bile duct repair using tissue engineering technique: PCL/PLGA bilayered scaffold with hMSCs. Journal of tissue engineering and regenerative medicine. 2017;11(4):966-76. doi:10.1002/term.1996.

14. Matsui M, Tabata Y. Enhanced angiogenesis by multiple release of platelet-rich plasma contents and basic fibroblast growth factor from gelatin hydrogels. Acta Biomater. 2012;8(5):1792-801. doi:10.1016/j.actbio.2012.01.016.

15. Nau P, Liu J, Ellison EC, Hazey JW et al. Novel reconstruction of the extrahepatic biliary tree with a biosynthetic absorbable graft. HPB (Oxford). 2011;13(8):573-8. doi:10.1111/j.1477-2574.2011.00337.x.

16. Li H, Chang J. Preparation and characterization of bioactive and biodegradable wollastonite/poly(D,L-lactic acid) composite scaffolds. Journal of materials science Materials in medicine. 2004;15(10):1089-95. doi:10.1023/B:JMSM.0000046390.09540.c2.

17. Taylor M, S.Daniels AU, Andriano KP, Heller J. Six bioabsorbable polymers: in vitro acute toxicity of accumulated degradation products. Journal of applied biomaterials : an official journal of the Society for Biomaterials. 1994;5(2):151-7. doi:10.1002/jab.770050208.

18. Suganuma J, Alexander H. Biological response of intramedullary bone to poly-L-lactic acid. Journal of Applied Biomaterials. 1993;4(1):13-27. doi:https://doi.org/10.1002/jab.770040103.

19. desJardins-Park HE, Foster DS, Longaker MT. Fibroblasts and wound healing: an update. Regenerative medicine. 2018;13(5):491-5. doi:10.2217/rme-2018-0073.

20. Saotome T, Shimada N, Matsuno K, Nakamura K, Tabata Y. Gelatin hydrogel nonwoven fabrics of a cell culture scaffold to formulate 3-dimensional cell constructs. Regen Ther. 2021;18:418-29. doi:10.1016/j.reth.2021.09.008.

21. Morell CM, Fabris L, Strazzabosco M. Vascular biology of the biliary epithelium. J Gastroenterol Hepatol. 2013;28 Suppl 1:26-32. doi:10.1111/jgh.12022.

22. Jinno C, Morimoto N, Ito R et al. A Comparison of Conventional Collagen Sponge and Collagen-Gelatin Sponge in Wound Healing. Biomed Res Int. 2016;2016:4567146. doi:10.1155/2016/4567146.

23. Chiu LL, Radisic M. Scaffolds with covalently immobilized VEGF and Angiopoietin-1 for vascularization of engineered tissues. Biomaterials. 2010;31(2):226-41. doi:10.1016/j.biomaterials.2009.09.039.

24. Luttikhuizen DT, Harmsen MC, Van Luyn MJ. Cellular and molecular dynamics in the foreign body reaction. Tissue engineering. 2006;12(7):1955-70. doi:10.1089/ten.2006.12.1955.

25. Xiao X, Wang W, Liu D et al. The promotion of angiogenesis induced by three-dimensional porous beta-tricalcium phosphate scaffold with different interconnection sizes via activation of PI3K/Akt pathways. Sci Rep. 2015;5:9409. doi:10.1038/srep09409.

26. Nagaike R, Sawaguchi A, Kawano J, Aoyama F, Oinuma T, Suganuma T. Regeneration of gastric mucosa during ulcer healing follows pathways that correspond to the ontogenetic course of rat fundic glands. Virchows Arch. 2004;445(6):580-8. doi:10.1007/s00428-004-1134-x.

27. Carpino G, Nevi L, Overi D et al. Peribiliary Gland Niche Participates in Biliary Tree Regeneration in Mouse and in Human Primary Sclerosing Cholangitis. Hepatology. 2020;71(3):972-89. doi:10.1002/hep.30871.

28. Sampaziotis F, Justin AW, Tysoe OC et al. Reconstruction of the mouse extrahepatic biliary tree using primary human extrahepatic cholangiocyte organoids. Nat Med. 2017;23(8):954-63. doi:10.1038/nm.4360.

29. Vashisht K, Nady SL, Engler RD et al. Extraparenchymal Bile/Pancreatic Ducts and Duodenal Papillae: Pathologic Evaluation in Nonclinical Species--A Brief Review. Toxicol Pathol. 2015;43(5):651-61. doi:10.1177/0192623314560612.

30. Yang J, Lu B. Establishment of a novel rat model of severe acute cholangitis. Iranian journal of basic medical sciences. 2015;18(11):1124-9.

31. Li WC, Zhang HM, Li J et al. Comparison of biomechanical properties of bile duct between pigs and humans for liver xenotransplant. Transplant Proc. 2013;45(2):741-7. doi:10.1016/j.transproceed.2012.11.006.

Tables

Table 1

Weight gain and biochemical values of preoperative and 12-week postoperative serum in the ABD and sham groups

	preoperative			12 weeks post-operative		
	sham group	ABD group	p value	sham group	ABD group	p value
Body weight (g)	260 ± 11.8	260 ± 11.0	1.000	340 ± 14.1	346 ± 13.6	0.670
T-Bil (mg/dL)	0.10 ± 0.00	0.14 ± 0.05	0.177	0.18 ± 0.04	0.16 ± 0.05	0.601
AST (IU/L)	68.4 ± 11.7	81.6 ± 21.4	0.463	69.4 ± 13.1	81.6 ± 28.0	0.676
ALT (IU/L)	35.8 ± 6.4	42.0 ± 5.2	0.173	32.4 ± 4.6	38.2 ± 3.2	0.074
ALP (IU/L)	545.2 ± 89.1	614.0 ± 119.1	0.403	351.6 ± 143.6	420.2 ± 146.2	0.403

n=5 (sham) and *n*=5 (ABD); data are presented as mean ± standard deviation, Mann–Whitney U test; ABD, artificial bile duct; T-Bil, total bilirubin; AST, aspartate transaminase; ALT, alanine aminotransferase; ALP, alkaline phosphatase

Table 2

Quantitative evaluation of bile duct epithelial regeneration

	re-epithelization ratio
2 weeks	10.4 ± 6.9 %
6 weeks	93.1 ± 5.1 %
12 weeks	99.2 ± 1.6 %

Data are presented as mean ± standard deviation

Figure legends

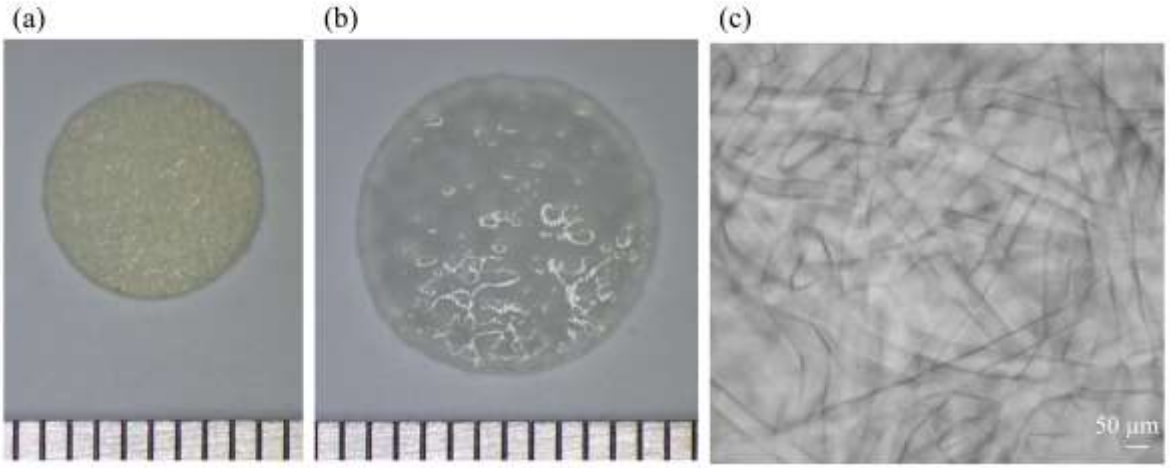

Figure 1. Macroscopic and microscopic appearance of the GHNF sheet.

a. dried GHNF sheet, b. swollen GHNF sheet, c. optical microscope image of the swollen GHNF sheet. Scale bar: 50 µm. GHNF, gelatin hydrogel non-woven fabrics

Tissue Engineering
Bile duct regeneration with an artificial bile duct made of gelatin hydrogel non-woven fabrics (DOI: 10.1089/ten.TEA.2021.0209)

Tissue Engineering
Bile duct regeneration with an artificial bile duct made of gelatin hydrogel non-woven fabrics (DOI: 10.1089/ten.TEA.2021.0209)

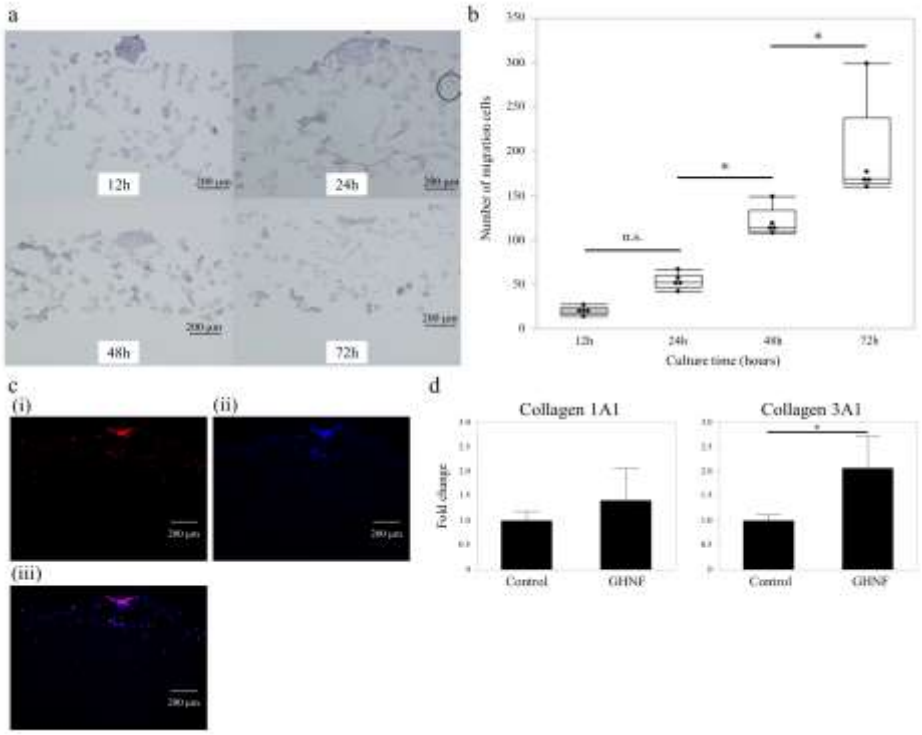

Figure 2. Migration and maintenance of cellular functions by murine L929 cells in the GHNF sheet.

a. Histology of the aggregates seeded on the GHNF sheet (Hematoxylin and eosin stain). Scale bar: 200 µm. b. Quantification of the number of migrating cells; *n*=5. Mann–Whitney U test. *p<0.05, n.s., not significant. **c.** Ki67 immunofluorescence 72 h after seeding the aggregates onto the GHNF sheet; (i) Ki67, (ii) DAPI, (iii) merge. Scale bar: 200 µm. **d.** Collagen mRNA expression in cultured L929 cells in the GHNF sheet. The control group was statically cultured L929 on a polyethylene dish for 3 d. *n*=5; error bar, standard deviation; Mann–Whitney U test; *p<0.05. GHNF, gelatin hydrogel non-woven fabrics, DAPI, 4,6-diamidino-2-phenylindole

Tissue Engineering
Bile duct regeneration with an artificial bile duct made of gelatin hydrogel non-woven fabrics (DOI: 10.1089/ten.TEA.2021.0209)

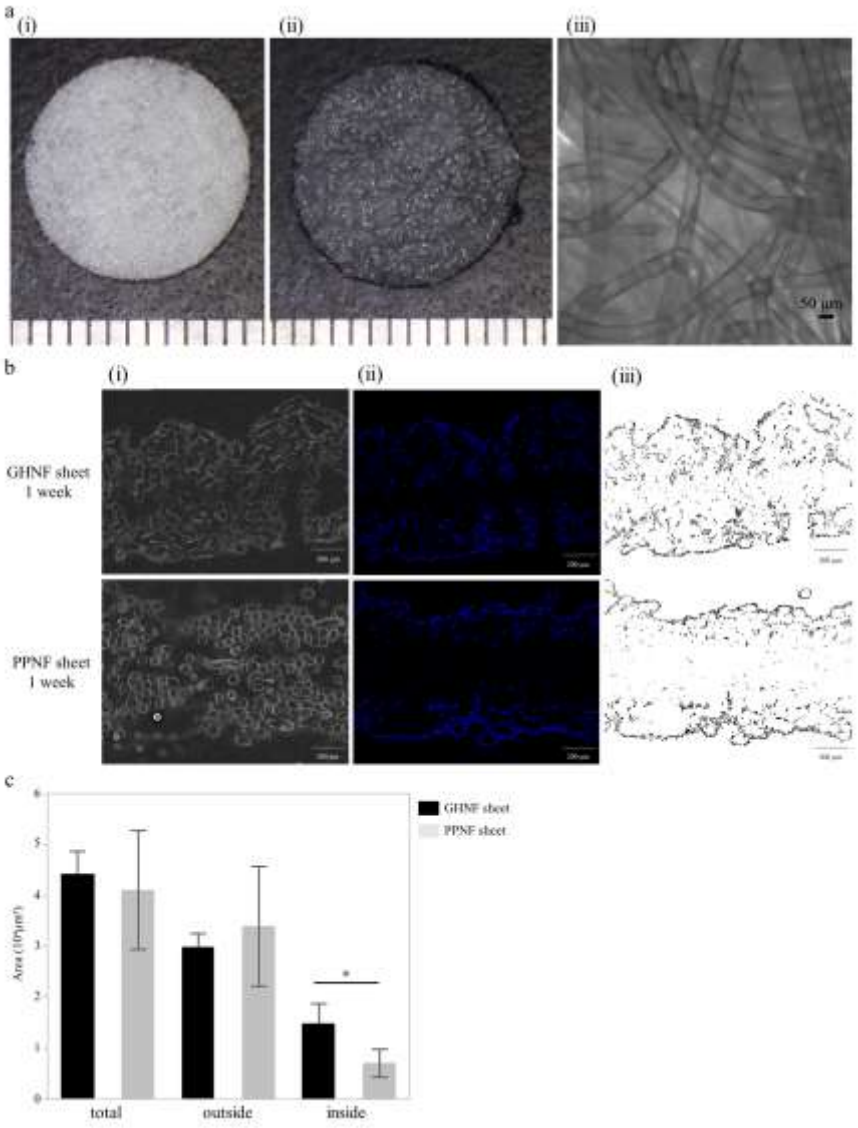

Figure 3. Comparison of cellular localization in the cultured GHNF and PPNF sheets.

a. Appearance of the PPNF sheet; (i) dried PPNF sheet, (ii) wet PPNF sheet, (iii) optical microscope image of the PPNF sheet. Scale bar: 50 μm. b. Localization of L929 cells cultured in the GHNF sheet or PPNF sheet 1 week after seeding. Images of (i) phase contrast microscopy and (ii) nuclear staining with DAPI; (iii) the image on the right was binarized with image analysis software. c. Area of seeded cells in the GHNF and the PPNF sheets; *n*=5; error bar, standard deviation; Mann–Whitney U test; *p<0.05. GHNF, gelatin hydrogel non-woven fabrics, PPNF, polypropylene non-woven fabric, DAPI, 4,6-diamidino-2-phenylindole

Tissue Engineering
Bile duct regeneration with an artificial bile duct made of gelatin hydrogel non-woven fabrics (DOI: 10.1089/ten.TEA.2021.0209)

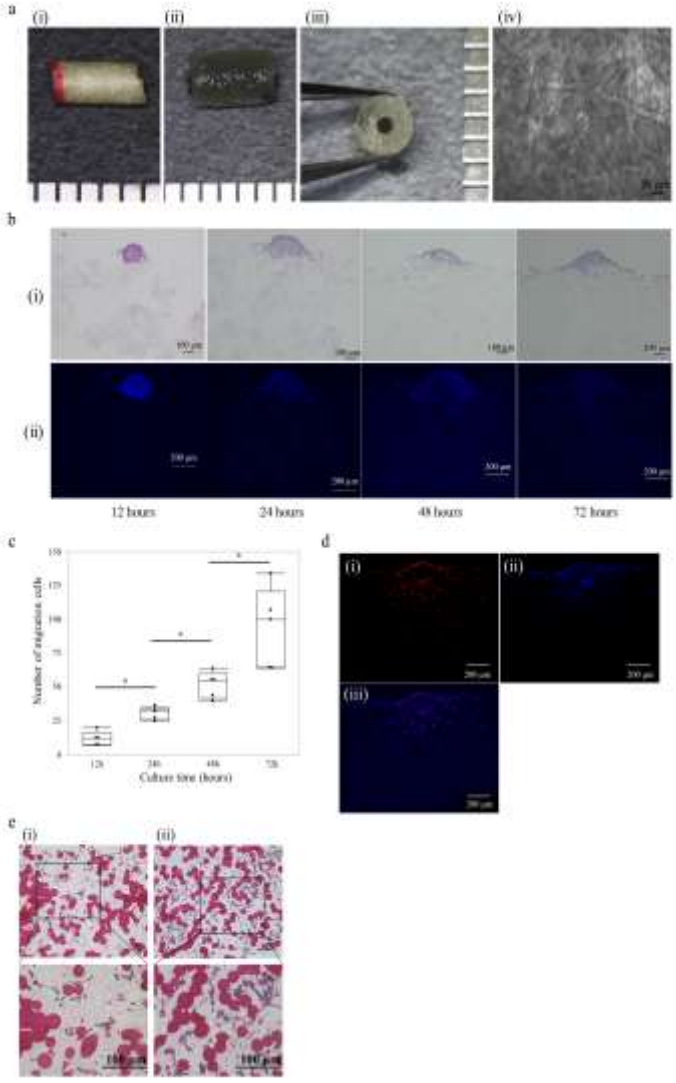

Figure 4. Cell migration and maintenance of cellular functions in the ABD.

a. Appearance of the ABD; (i) dried ABD, (ii) swollen ABD, (iii) cross section of the swollen ABD, (iv) optical microscope image of the swollen ABD. Scale bar: 50 µm. b. Histology of the aggregates seeded on ABD; (i) Hematoxylin and eosin stain, (ii) nuclear staining with DAPI. Scale bars: (i) 100 µm, (ii) 200 µm c. Quantification of number of migrating cells; *n*=5; Mann–Whitney U test; *p<0.05 d. Immunofluorescence of Ki67 72 h after seeding the aggregates on the ABD; (i) Ki67, (ii) DAPI, (iii) merge. Scale bar: 200 µm. e. Images of Sirius Red/Fast Green staining of ABD cultured for (i) 1 or (ii) 2 weeks. Scale bar: 100 µm. ABD, artificial bile duct, DAPI, 4,6-diamidino-2-phenylindole

Tissue Engineering
Bile duct regeneration with an artificial bile duct made of gelatin hydrogel non-woven fabrics (DOI: 10.1089/ten.TEA.2021.0209)

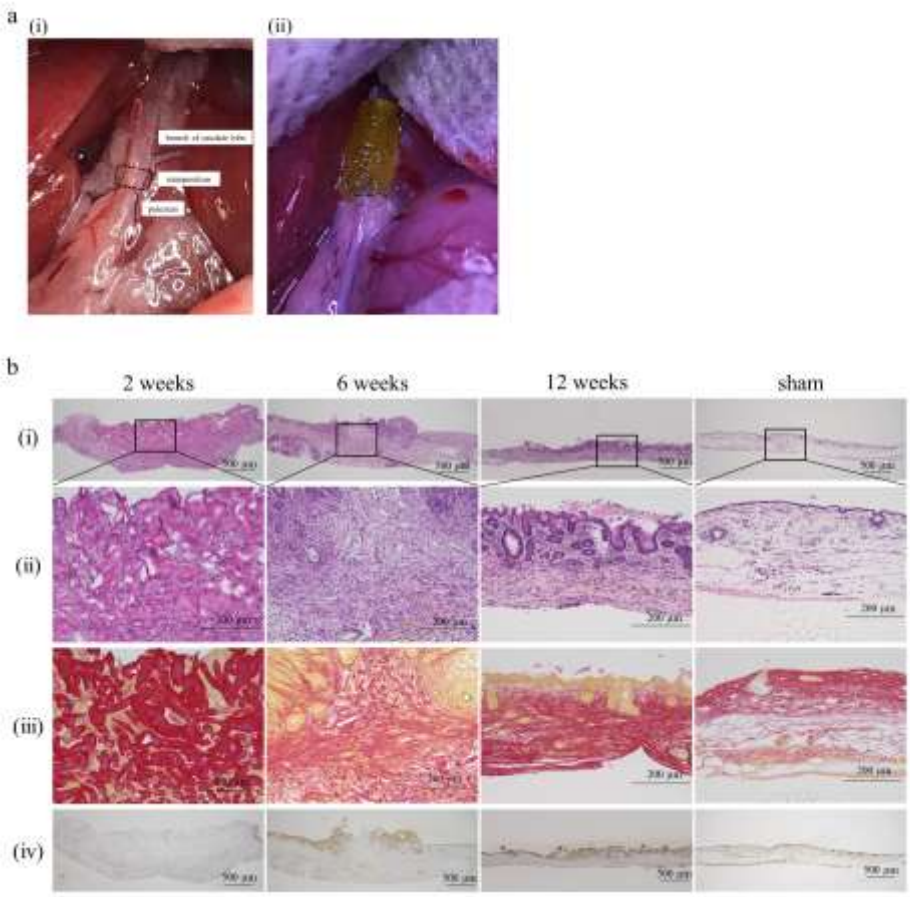

Figure 5. Surgical findings of ABD implantation and histopathology of the ABD implantation site and liver over time.

a. Surgical findings of ABD implantation; (i) pre-operation, (ii) post-operation. The extrahepatic bile duct between the branch of the caudate lobe and the tail of the pancreas was excised and connected with ABD (length: 4 mm). b. Histopathology at the ABD implantation site over time; (i) 40×, (ii) 200× magnifications of Hematoxylin and eosin staining, (iii) Sirius red staining, (iv) Cytokeratin 19 immunohistochemistry. Scale bars: (i) (iv) 500 µm, (ii) (iii) 200 µm. ABD, artificial bile duct

Tissue Engineering
Bile duct regeneration with an artificial bile duct made of gelatin hydrogel non-woven fabrics (DOI: 10.1089/ten.TEA.2021.0209)

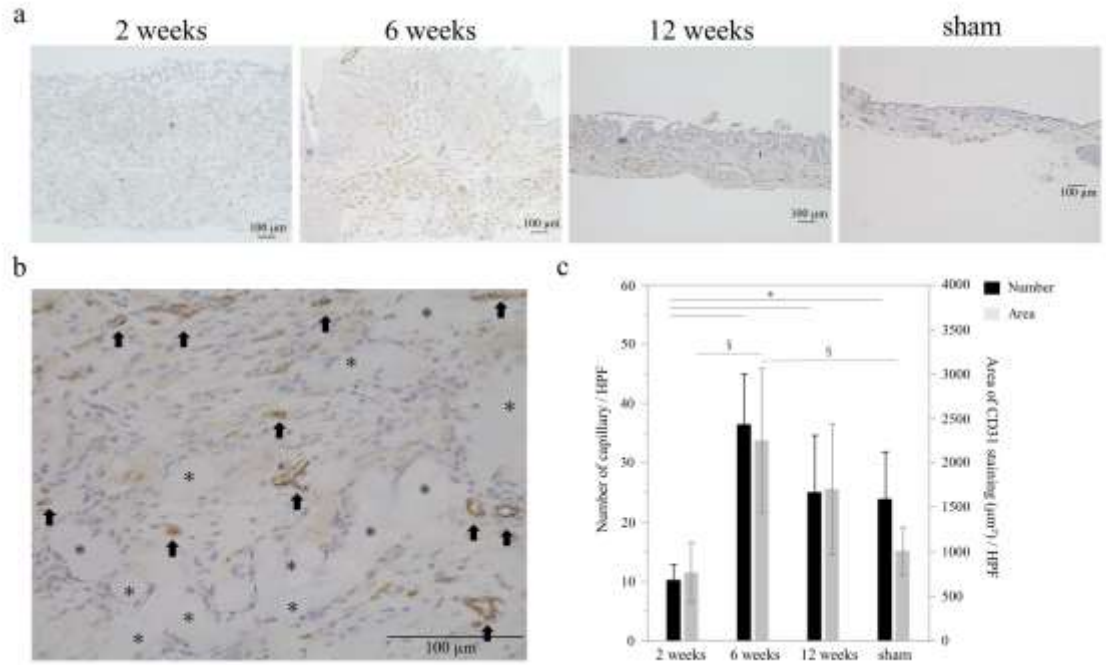

Figure 6. Angiogenesis within the ABD rat implantation model.

a. CD31 immunohistochemistry in the ABD 2, 6, and 12 weeks after implantation and in the sham group. Scale bar: 100 μm. b. High-power magnification of CD31 immunohistochemistry in the ABD 2 weeks after implantation. Black arrow shows CD31 positive vascular structures; * shows gelatin fibers; scale bar: 100 μm. c. Quantification of the number of capillaries and the CD31-positive area at the implantation site; *n*=5 (2 weeks), *n*=4 (6 weeks), *n*=5 (12 weeks), and *n*=5 (sham group). Mann–Whitney U test. *p-value for the number of capillaries <0.05; §p-value for the area of CD31 staining <0.05. ABD, artificial bile duct

Tissue Engineering
Bile duct regeneration with an artificial bile duct made of gelatin hydrogel non-woven fabrics (DOI: 10.1089/ten.TEA.2021.0209)

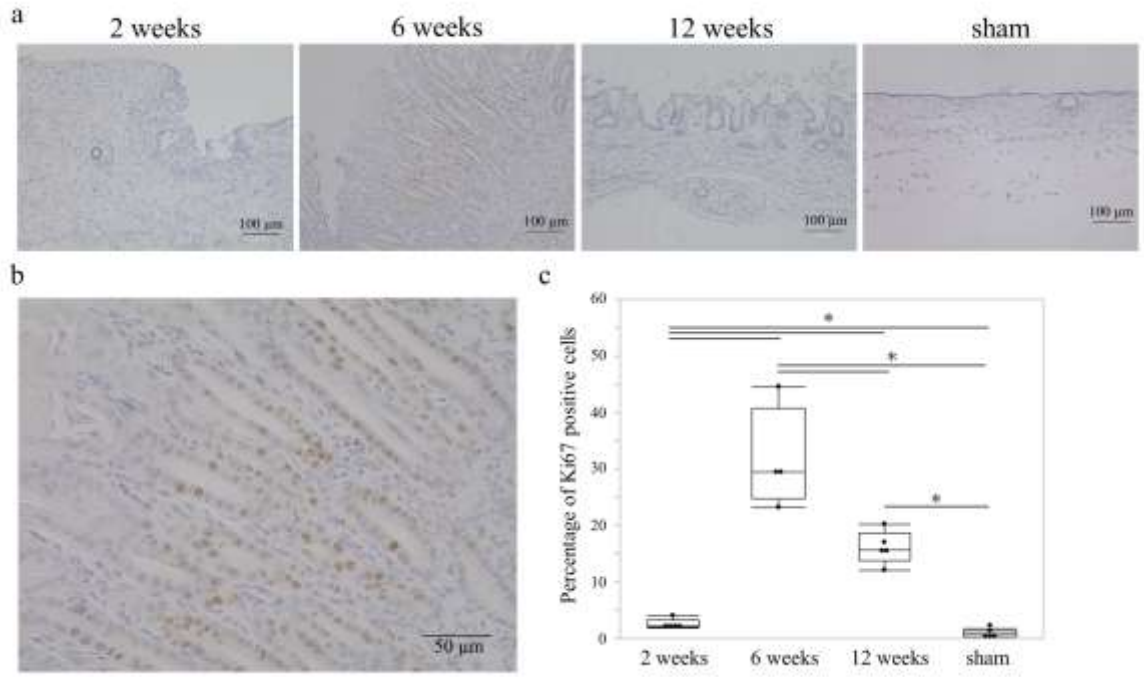

Figure 7. Proliferation of biliary epithelial cells in the rat implantation model.

a. Ki67 immunohistochemistry of the ABD 2, 6, and 12 weeks after implantation and in the sham group. Scale bar: 100 μm. b. High-power magnification of Ki67 immunohistochemistry of the ABD 6 weeks after implantation. Scale bar: 50 μm. c. Quantification of the percentage of Ki67 positive cells. *n*=5 (2 weeks), *n*=4 (6 weeks), *n*=5 (12 weeks), and *n*=5 (sham). Mann–Whitney U test; *p<0.05. ABD, artificial bile duct